Immunity-related GTPase induces lipophagy to prevent excess hepatic lipid accumulation

Kristin Schwerbel, Anne Kamitz, Natalie Krahmer, Nicole Hallahan, Markus Jähnert, Pascal Gottmann, Sandra Lebek, Tanja Schallschmidt, Danny Arends, Fabian Schumacher, Burkhard Kleuser, Tom Haltenhof, Florian Heyd, Sofiya Gancheva, Karl W. Broman, Michael Roden, Hans-Georg Joost, Alexandra Chadt, Hadi Al-Hasani, Heike Vogel, Wenke Jonas, Annette Schürmann

Table of contents

Supplementary figures

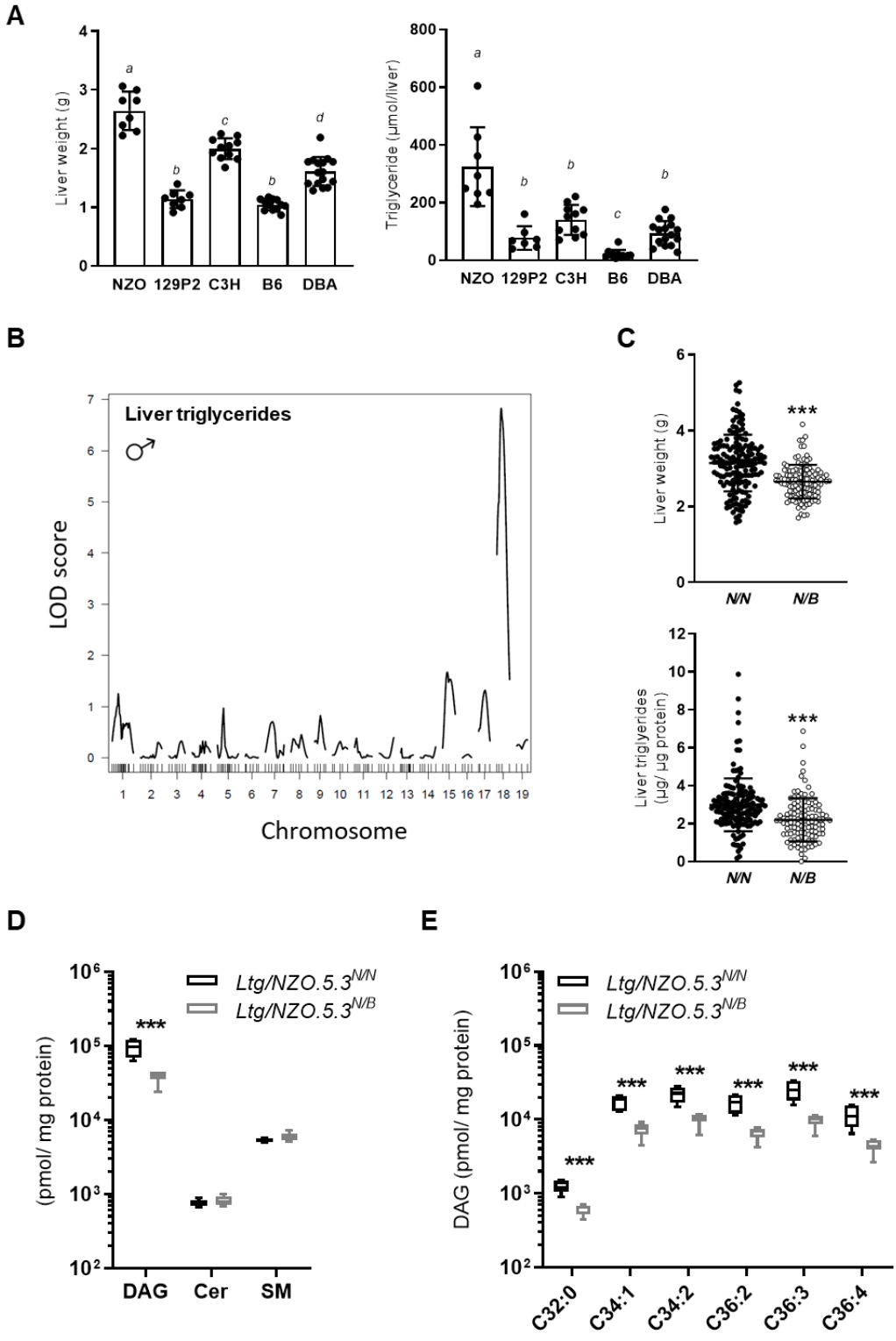

Fig. S1. Analysis of hepatic lipid levels and different lipid species. (A) Liver weight and triglyceride concentrations of NZO (n=8), B6 (n=12), DBA (n=16), C3H (n=11) and 129P2 (n=8) mice. Data analyzed by Kruskal-Wallis test and presented as mean ± SD. Data not marked with the same letter are significantly different. (B) Genome-wide linkage analysis of male mice of the (NZOxB6)N2 population at 16 weeks of age for the trait liver triglycerides with a non-parametric model. (C) Effects of the genotype at SNP rs4231907 (17 cM) on liver weight and liver triglycerides (*N/N*=143-159; *N/B*=109-119). Data analyzed by unpaired *t*-test with Welch´s correction and presented as mean ± SD. (D) Overall concentrations of hepatic diacylglycerols (DAG), ceramides (Cer) and sphingomyolins (SM) in livers of *Ltg/NZO.5.3*$^{N/N}$ (n=7) and *Ltg/NZO.5.3*$^{N/B}$ (n=9) mice. (E) Profile of single DAG species with corresponding fatty acid residues. Data analyzed by unpaired *t* test with Welch´s correction. Values are median (line), upper- and lower quartile (box) and extremes (whiskers). ****p*<0.001.

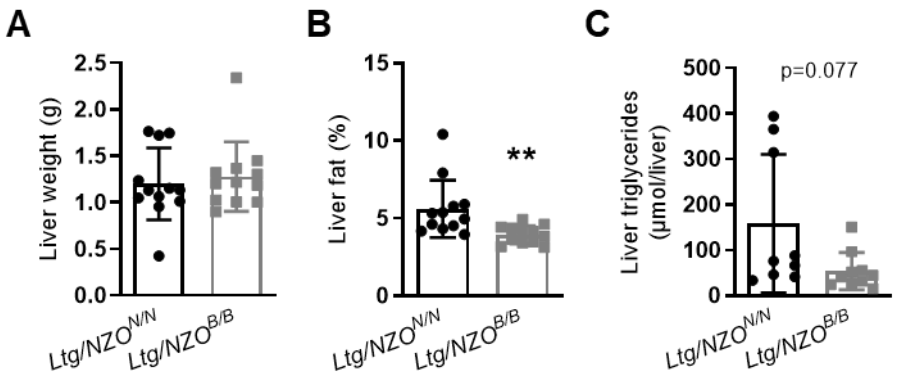

Fig. S2. Effect of *Ltg/NZO* is independent of adipogenic state of the animals. (A) Analysis of homozygous NZO- and B6-allele carriers (*Ltg/NZO*$^{N/N}$, *Ltg/NZO*$^{B/B}$) on the genetic background of B6 mice. (A) Liver weight (n=12), (B) liver fat content detected by computed tomography (n=12) and (C) liver triglyceride levels (*N/N*:n=9; *B/B*: n=10). Data analyzed by unpaired *t* test with Welch´s correction and presented as mean ± SD. ***p*<0.01.

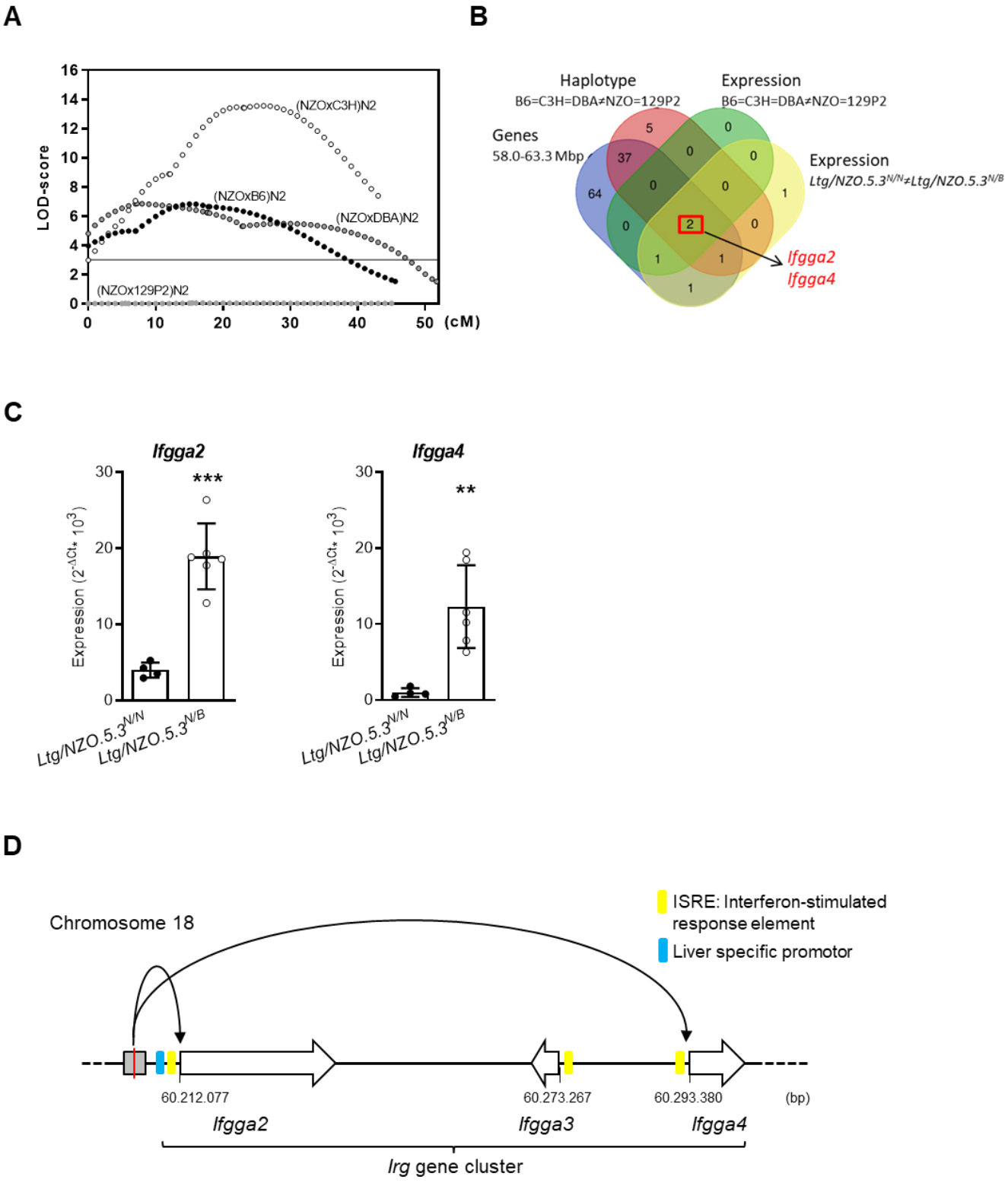
A
LOD-score
(NZOxC3H)N2
(NZOxB6)N2
(NZOxDBA)N2
(NZOx129P2)N2
(cM)
B
Haplotype
B6=C3H=DBA≠NZO=129P2
Expression
B6=C3H=DBA≠NZO=129P2
Genes
58.0-63.3 Mbp
Expression
Ltg/NZO.5.3N/N≠Ltg/NZO.5.3N/B
Ifgga2
Ifgga4
C
Ifgga2
Ifgga4
Expression (2-ΔCt* 103)
Ltg/NZO.5.3N/N
Ltg/NZO.5.3N/B
D
Chromosome 18
ISRE: Interferon-stimulated response element
Liver specific promotor
60.212.077
60.273.267
60.293.380
(bp)
Ifgga2
Ifgga3
Ifgga4
Irg gene cluster

Fig. S3. Identification of *Ifgga2* and *Ifgga4* as responsible gene variants. (A) The *Ltg/NZO* is present in the (NZOxB6)N2, (NZOxC3H)N2 and (NZOxDBA2)N2 but absent in the (NZOx129P2)N2 progeny, suggesting that the causal genomic variants of the locus of B6, C3H and DBA share common alleles which are different to NZO and 129P2. (B) Venn diagram including the total number of annotated genes in the critical region (left), number of genes from haplotype analysis (upper left) and microarray analysis of parental (upper right) and recombinant congenic mice (right) as well as the final overlap (red box). (C) Expression of *Ifgga2* and *Ifgga4* in liver of recombinant congenic mice (*Ltg/NZO*$^{N/N}$ [n=4], *Ltg/NZO*$^{N/B}$ [n=6]). Data were normalized to *Ppia*. Data analyzed by unpaired *t* test with Welch´s correction and presented as mean ± SD. **p<0.01; ***p<0.001. (D) Model for the regulation of the *Irg* gene cluster on chromosome 18.

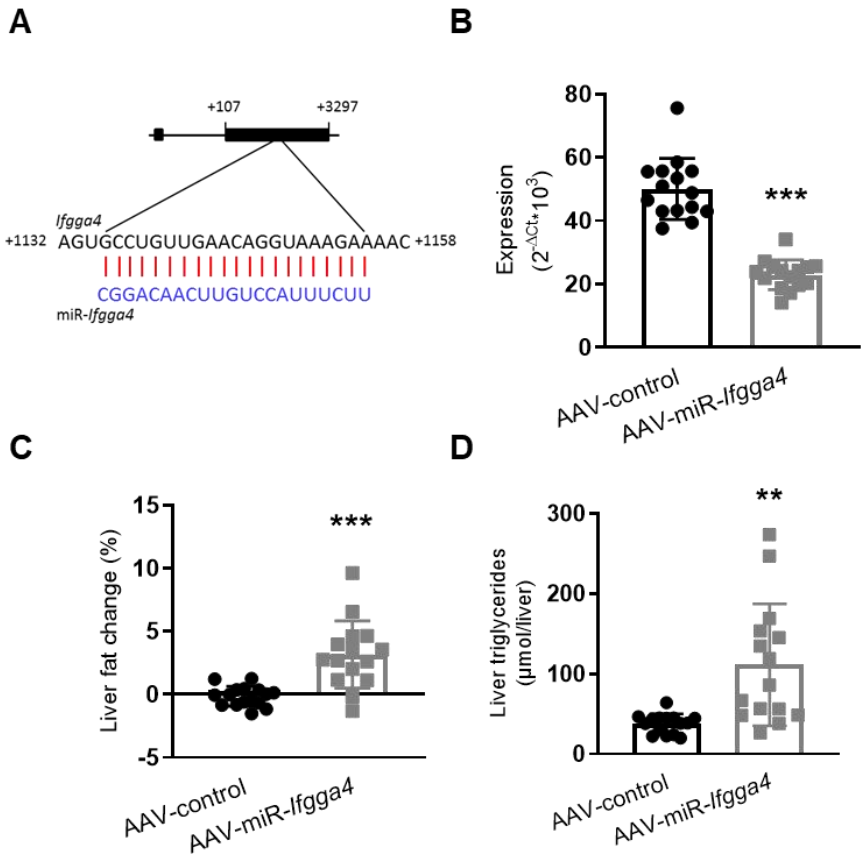
A
+107
+3297
Ifgga4
+1132 AGUGCCUGUUGAACAGGUAAAGAAAAC +1158
CGGACAACUUGUCCAUUUCUU
miR-Ifgga4
B
Expression
(2^-ΔCt*10^3)
80
60
40
20
0
***
AAV-control
AAV-miR-Ifgga4
C
Liver fat change (%)
15
10
5
0
-5
***
AAV-control
AAV-miR-Ifgga4
D
Liver triglycerides
(μmol/liver)
300
200
100
0
**
AAV-control
AAV-miR-Ifgga4
E
AAV-control
AAV-miR-Ifgga4
20μM
20μM
50μm
50μm

Fig. S4. Hepatocyte specific suppression of *Ifgga4* in B6 mice. (A) Sequence of the designed miRNA and the targeted sequence of *Ifgga4.* (B) Hepatic expression of *Ifgga4* in AAV-control or AAV-miR-*Ifgga4* mice (n=16; normalized to *Ppia*). (C) Change of liver fat detected by computed tomography and (D) hepatic triglyceride levels 8 weeks after virus injection (n=15). (E) Detection of PLIN2 (green) and nuclei (TO-PRO, blue) in liver sections as well as H&E staining. Data analyzed by unpaired *t* test with Welch´s correction and presented as mean ± SD. ***p*<0.01; ****p*<0.001.

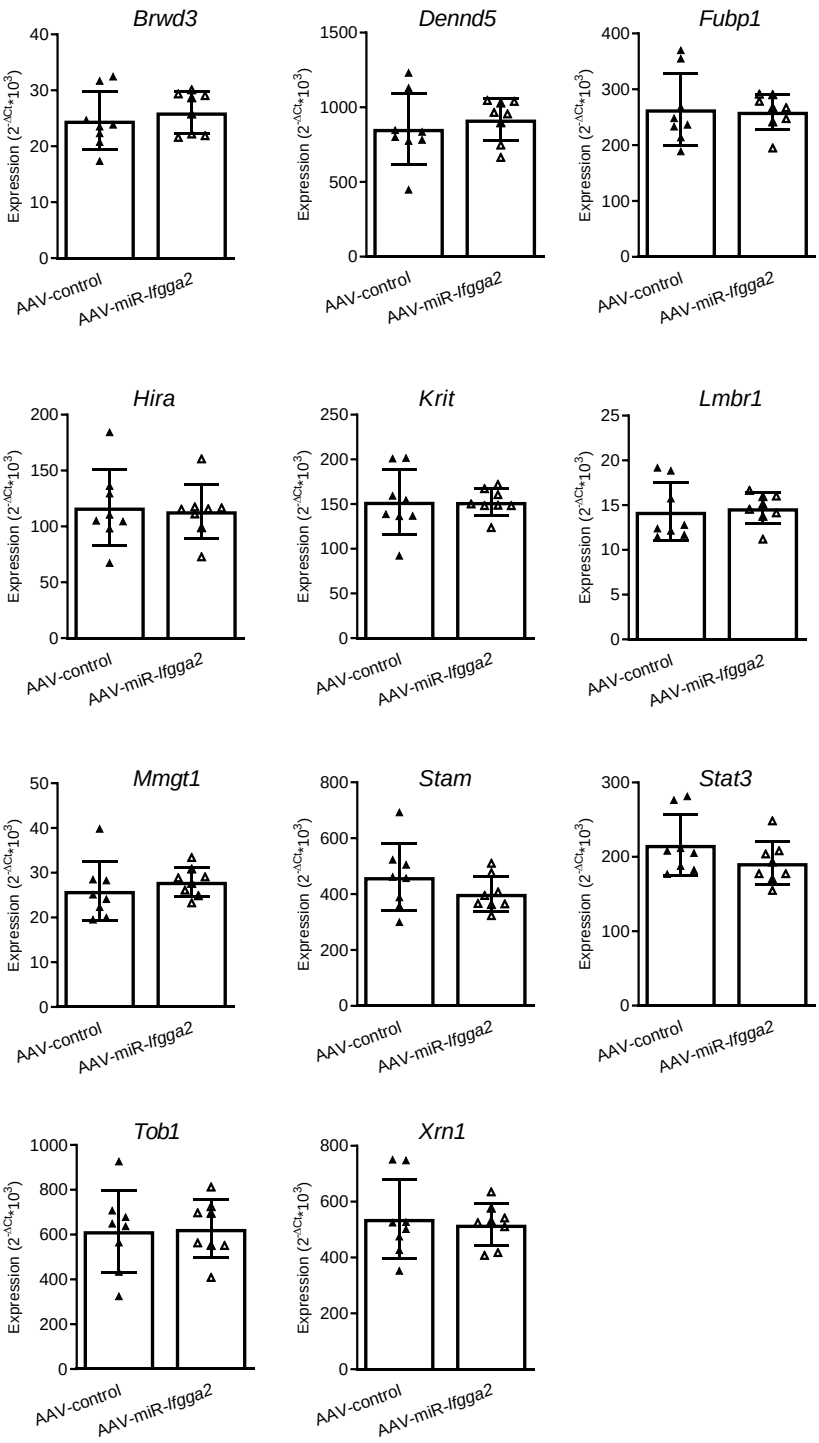

Fig. S5. Expression analysis of putative target genes of miR-*Ifgga2*. mRNA expression of 11 putative target genes of miR-*Ifgga2* in livers of AAV-control and AAV-miR-*Ifgga2* mice (n=8). Data analyzed by unpaired *t* test with Welch´s correction and presented as mean ± SD.

A McArdle hepatocytes

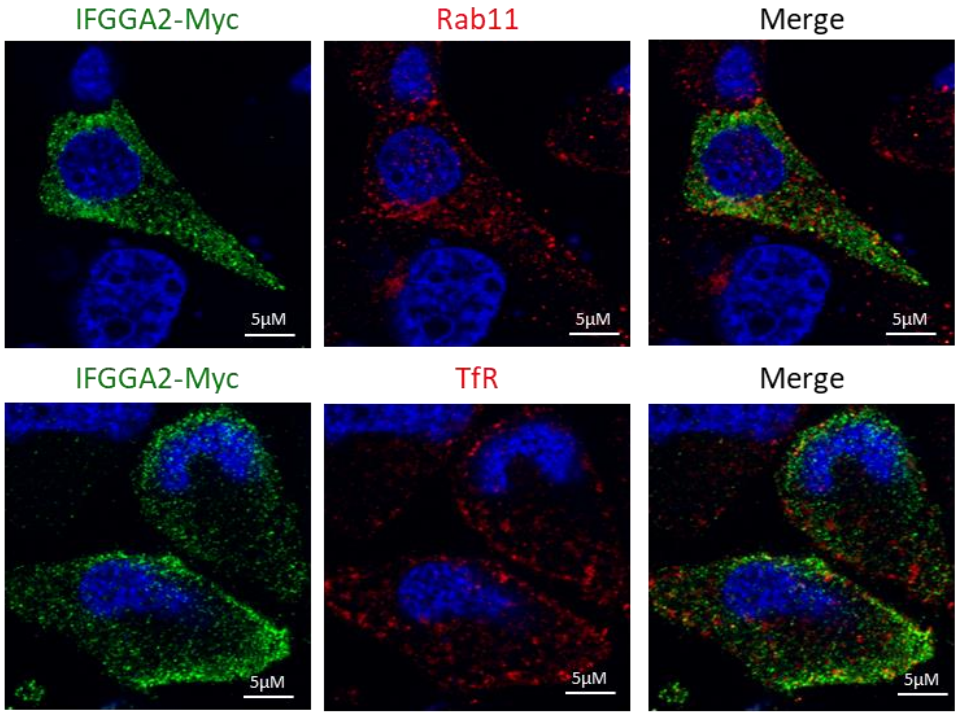

B HeLa cells

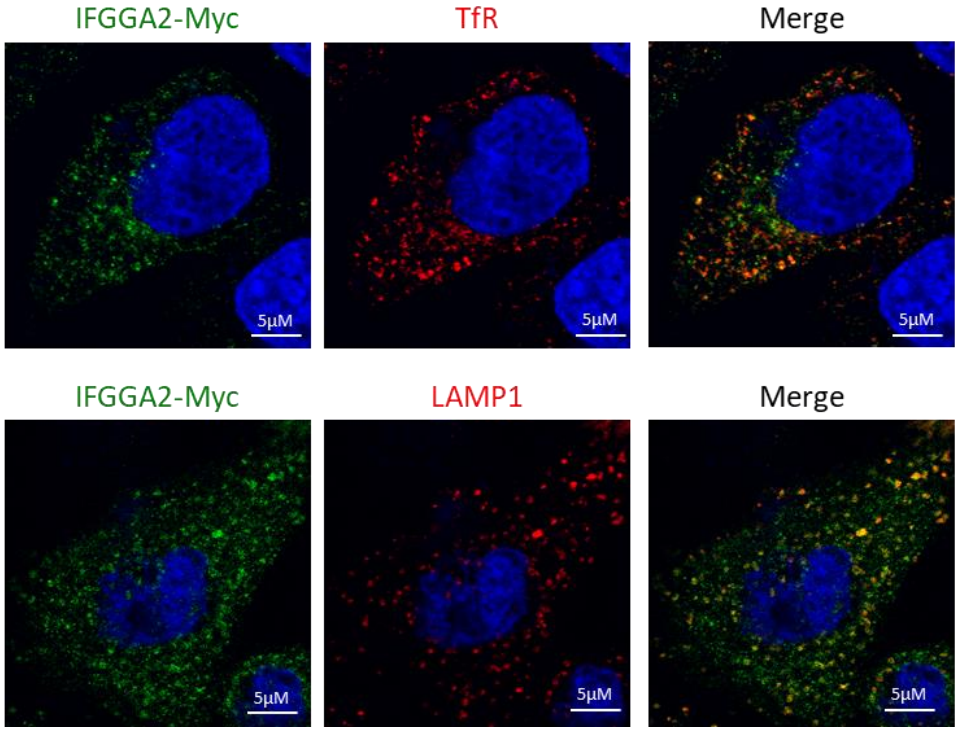

Fig. S6. Co-staining of IFGGA2 with endosomal and lysosomal marker proteins. (A) Immunocytochemical staining of Rab11 and transferrin receptor (TfR) in McArdle hepatocytes after IFGGA2-Myc overexpression. (B) Co-staining of TfR and LAMP1 with IFFGA2-Myc in HeLa cells.

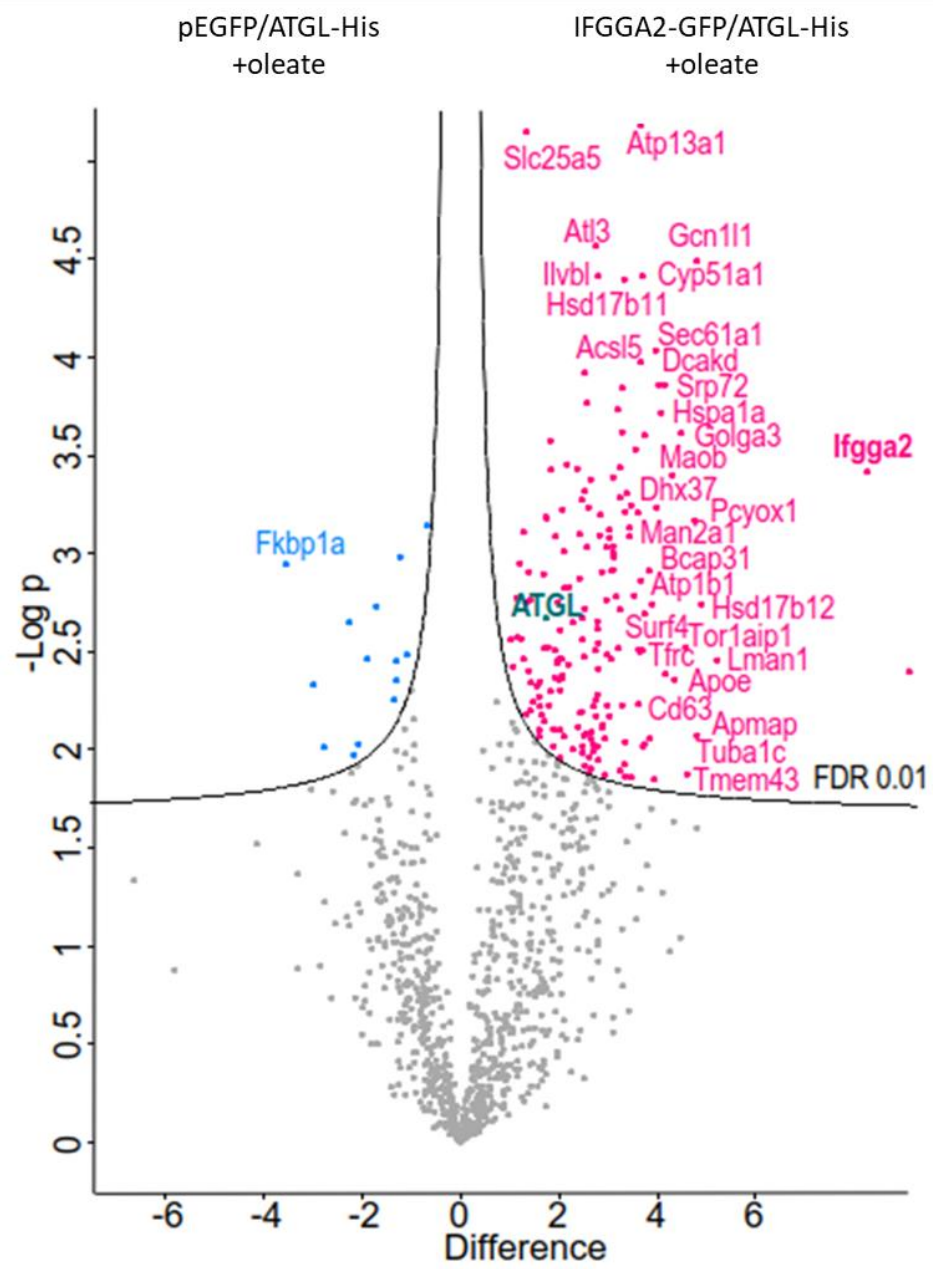

Fig. S7. Mass spectrometry-based proteomic analysis identified ATGL as interacting partner of IFGGA2. Volcano plot of mass spectrometry-based proteomic analysis of GFP-pulldown in oleate treated McArdle hepatocytes transfected with pEGFP+ATGL-His or IFGGA2-GFP+ATGL-His. IFGGA2 and ATGL are significantly enriched in pulldown from cells expressing IFFGA2-GFP compared to control cells transfected with GFP alone.

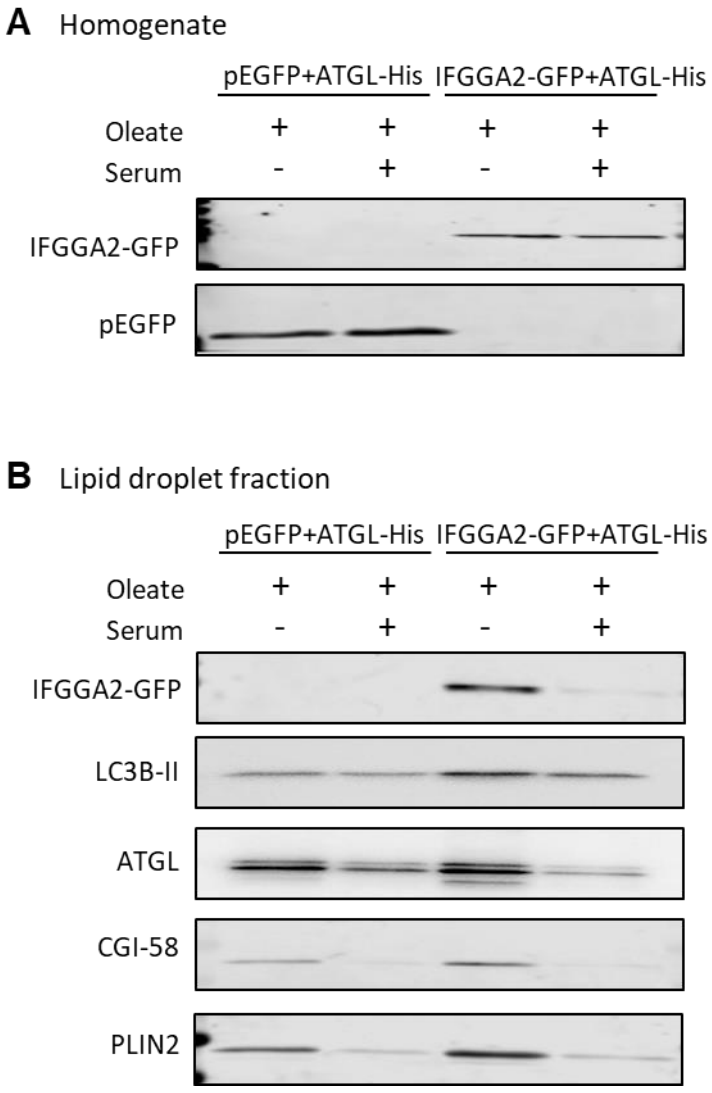

Fig. S8. Higher levels of LC3B-II in lipid droplet fraction of IFGGA2-overexpressing hepatocytes. (A) Western blotting of GFP of homogenates from McArdle hepatocytes overexpressing either pEGFP+ATGL-His or IFGGA2-GFP+ATGL-His. (B) Western blotting of GFP, LC3B-II, ATGL, CGI-58, and PLIN2 in lipid droplet fractions of McArdle hepatocytes overexpressing either pEGFP+ATGL-His or IFGGA2+ATGL-His.

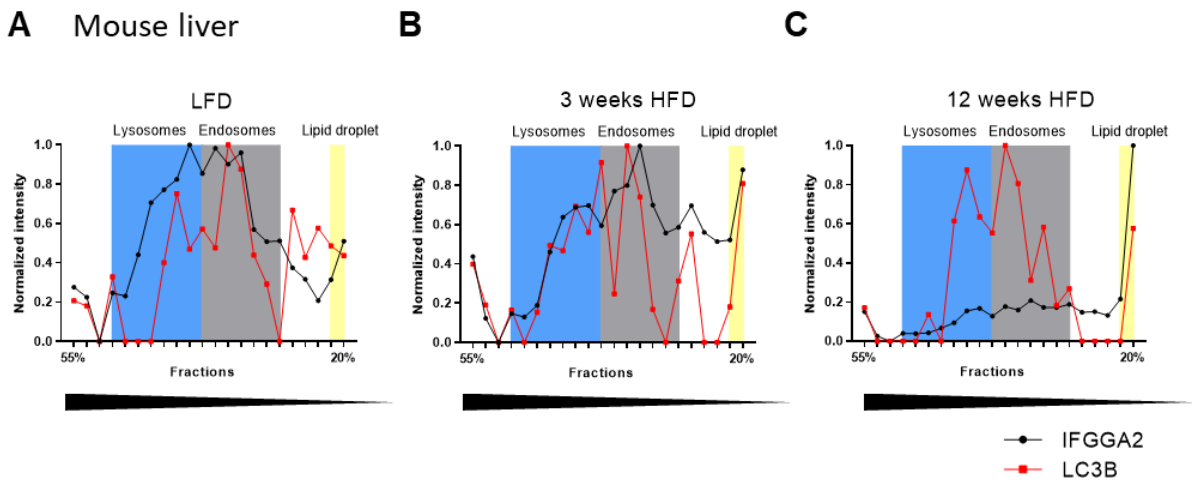

Fig. S9. Diet-dependent changes of IFGGA2 and LC3B localization in liver fractions of mice. Localization of IFGGA2 and LC3B upon (A) LFD or HFD feeding for (B) 3 or (C) 12 weeks. X-axis: Percentage of sucrose gradient. Y-axis: Normalized intensity of IFGGA2 and LC3B in isolated fractions.

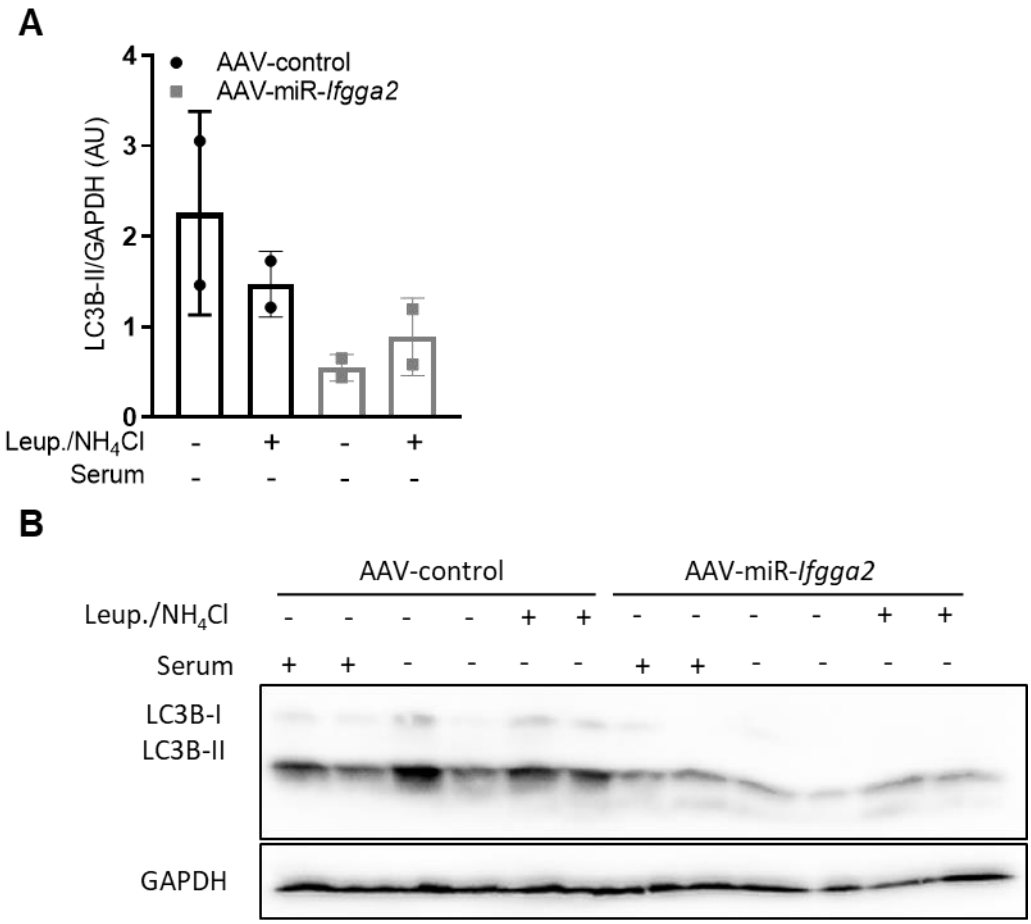
A
AAV-control
AAV-miR-lfgga2
LC3B-II/GAPDH (AU)
0
1
2
3
4
Leup./NH4Cl - + - +
Serum - - - -
B
AAV-control
AAV-miR-lfgga2
Leup./NH4Cl - - - - + + - - - - + +
Serum + + - - - - + + - - - -
LC3B-I
LC3B-II
GAPDH
C
AAV-control
AAV-miR-lfgga2
LC3B-II/GAPDH (AU)
0
1
2
3
4
Leup./NH4Cl - + - +
Serum - - - -

Fig. S10. Reduced autophagy upon hepatic *Ifgga2* suppression. (A) Downregulation of *Ifgga2* in primary hepatocytes 48h after siRNA transfection. mRNA levels were normalized to *β-actin* (n=2). (B) *Ex vivo* autophagy flux assay from liver explants of AAV-control and AAV-miR-*Ifgga2* mice. Western blot analysis and (C) corresponding quantification. Data analyzed by Kruskal-Wallis test and presented as mean ± SD.

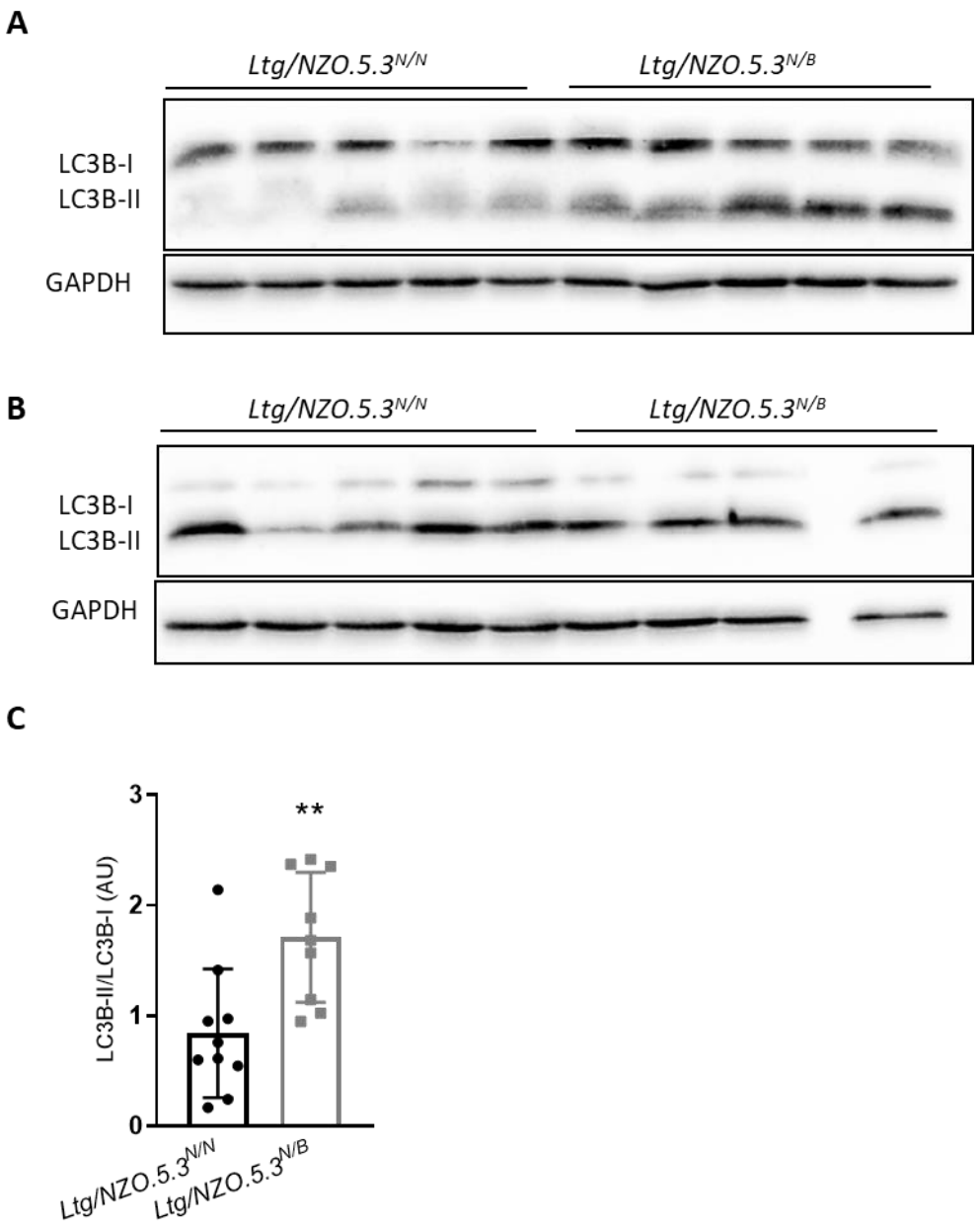

Fig. S11. Lower levels of *Ifgga2* reduced autophagy in the liver. (A,B) Analysis of LC3B-II in livers of *Ltg/NZO.5.3$^{N/N}$* (n = 10) and *Ltg/NZO.5.3$^{N/B}$* (n = 9) mice after 16h fasting. (C) Quantification of signal intensity by densitometric analysis and expressed as fold of control (*N/N*). Data analyzed by unpaired *t* test with Welch´s correction and presented as mean ± SD. ***p*<0.01

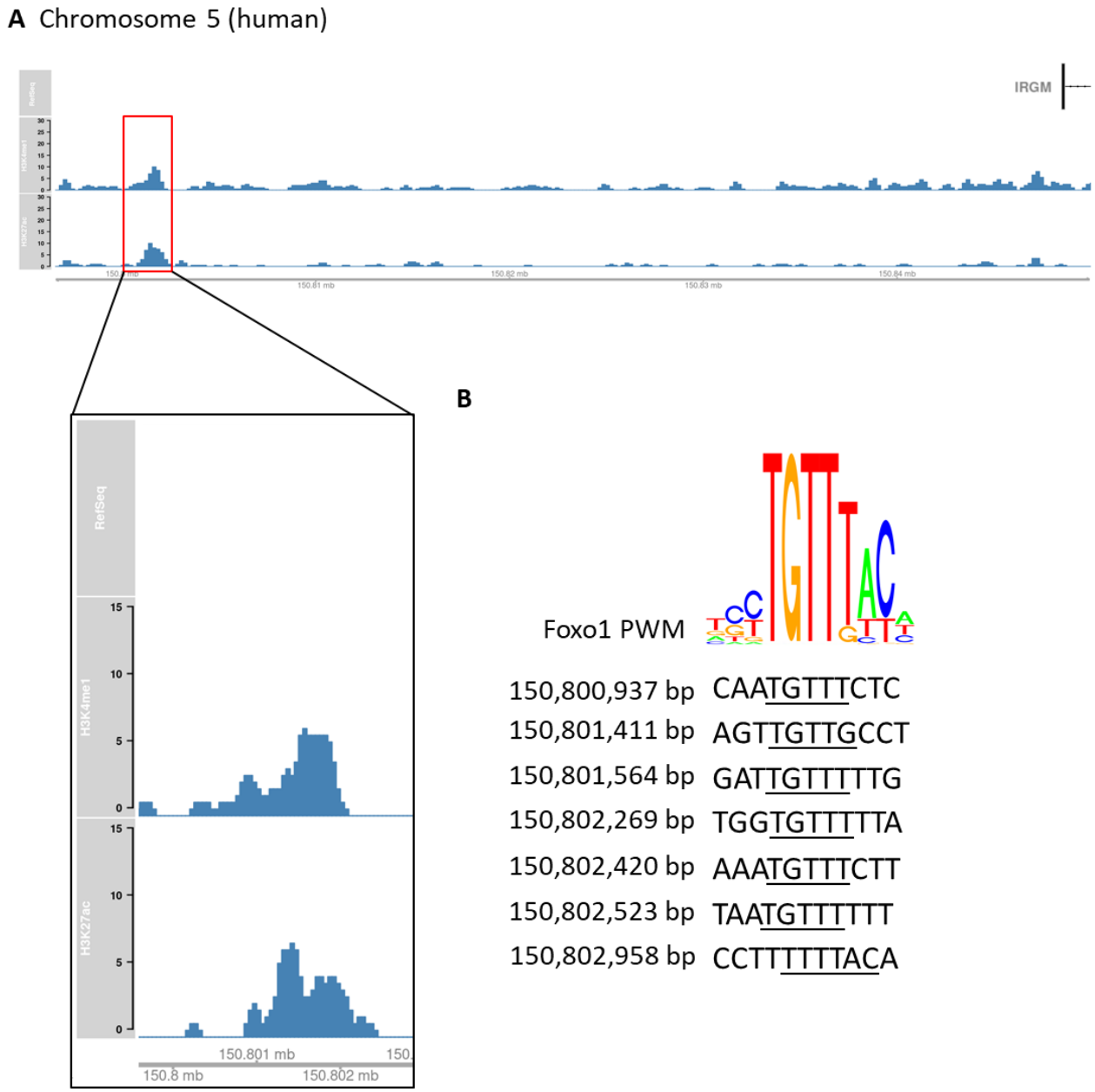

Fig. S12. Putative Foxo1 binding motifs in active enhancer elements upstream of *IRGM*. (A) Identification of binding sites for transcription factor Foxo1 within 50 kb upstream of transcription start site of *IRGM*. Active enhancers marked by histone modifications (H3K27Ac, H3K4me1). (B) Position weight matrix (PWM) of putative Foxo1 binding sites.

Original Western blots

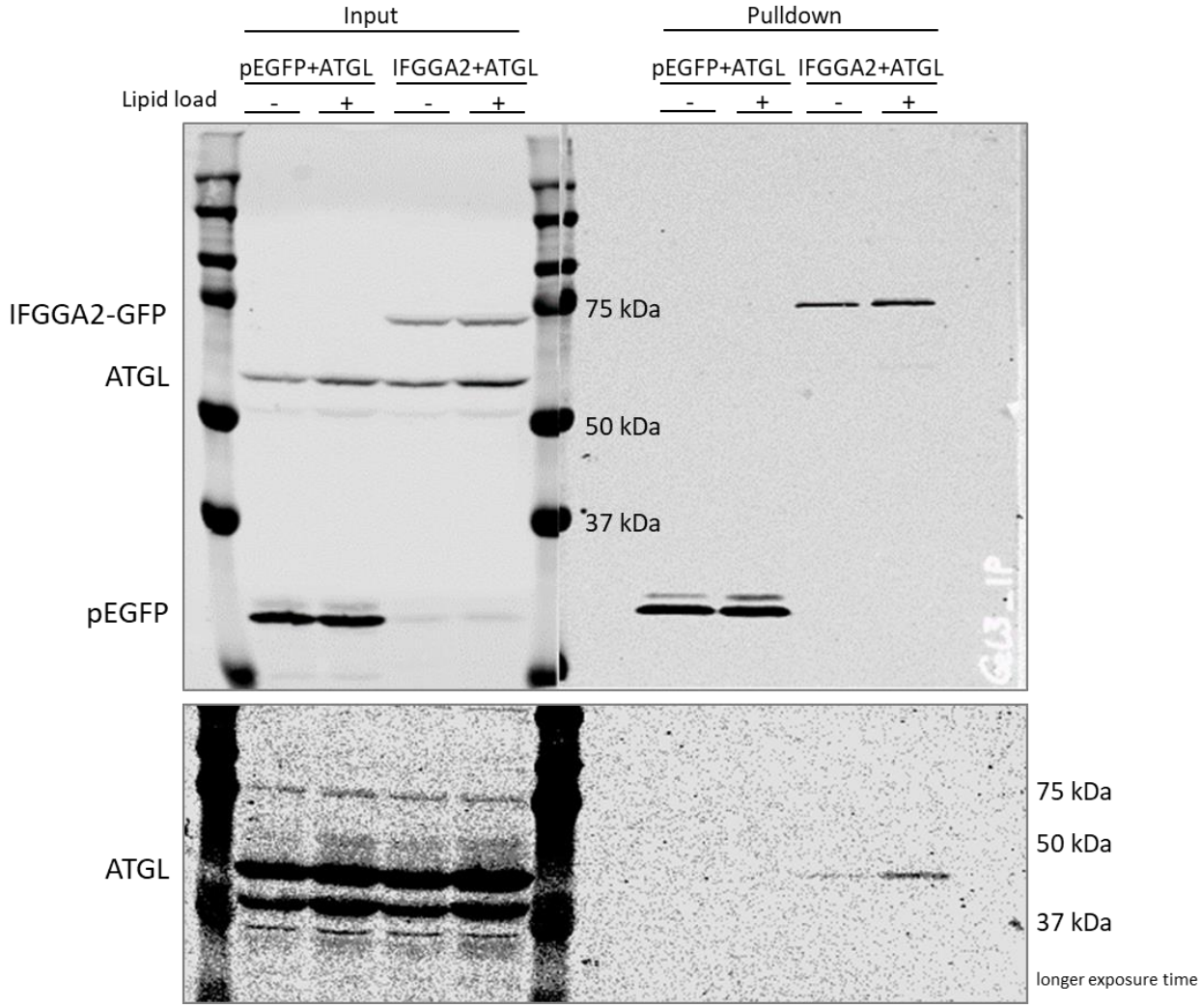

Fig. S13. Uncropped Western blots related to figure 5B.

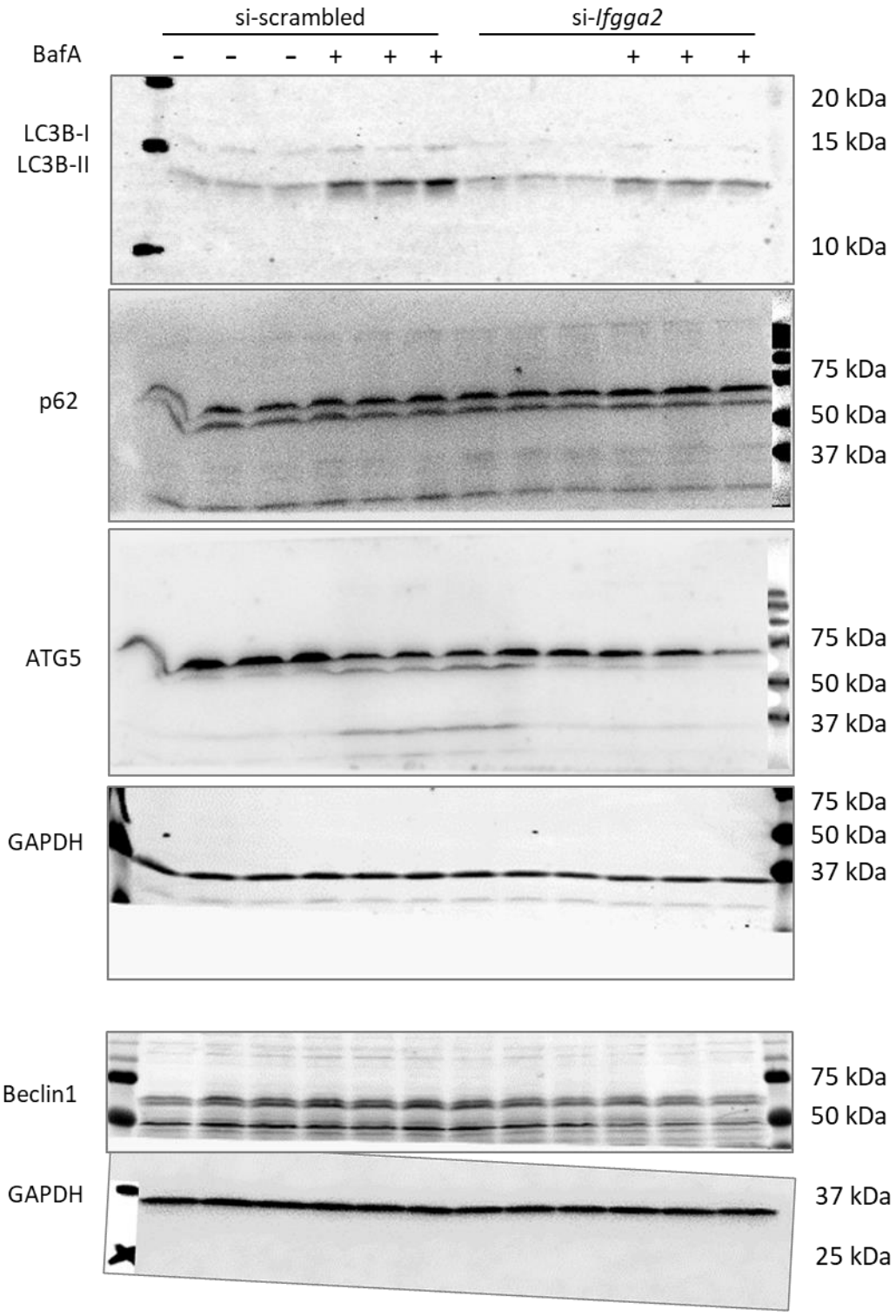

Fig. S14. Uncropped Western blots related to figure 6A.

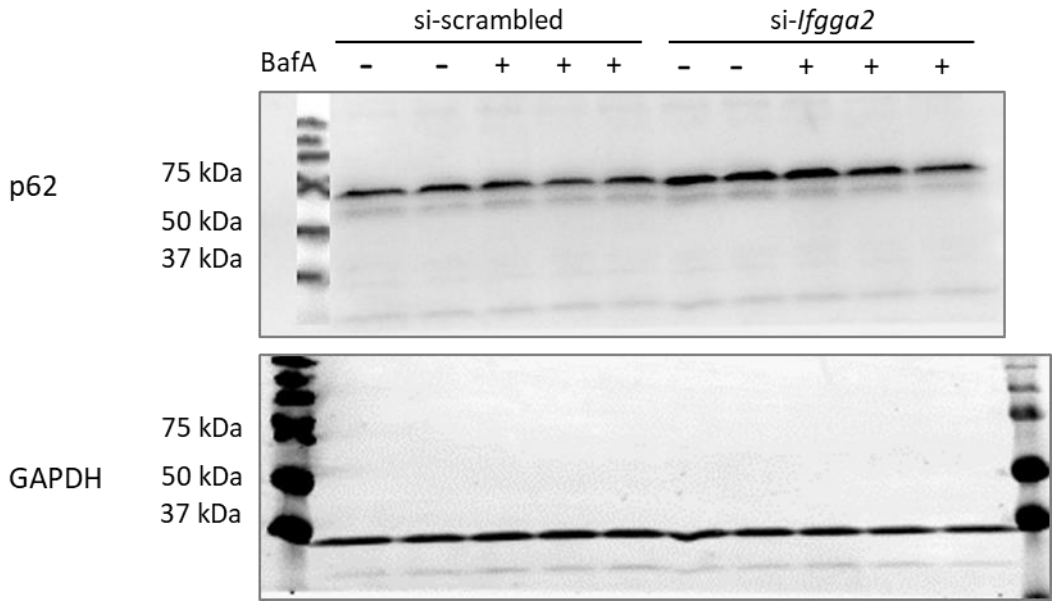

Fig. S15. Uncropped Western blots related to figure 6B.

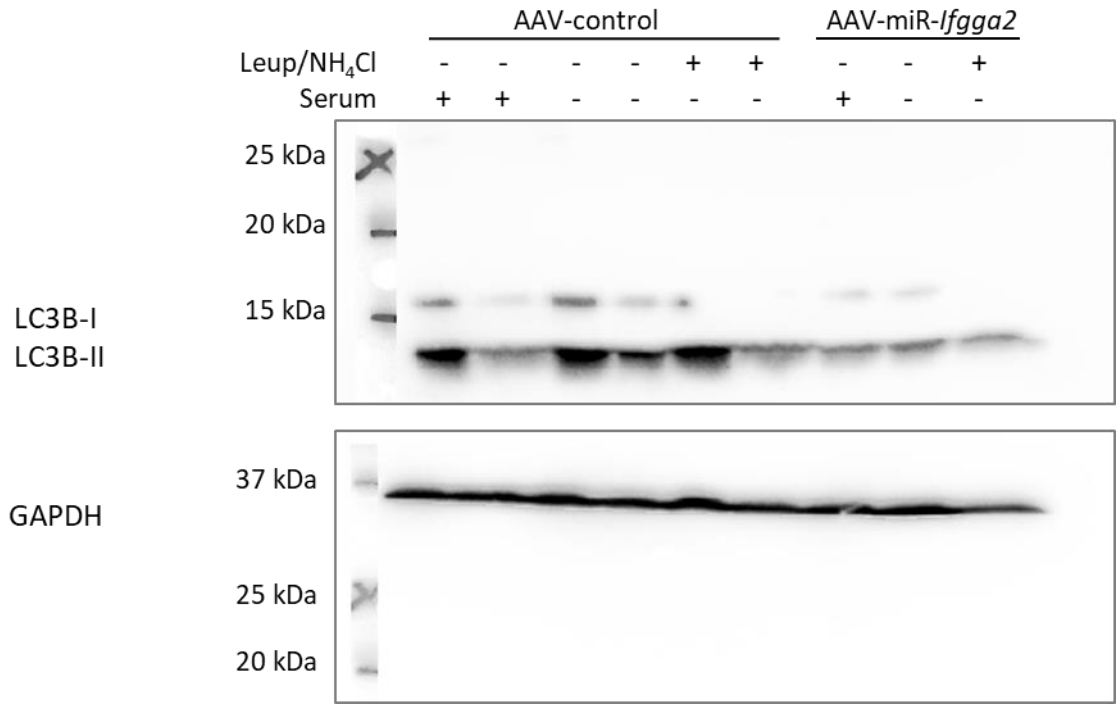

Fig. S16. Uncropped Western blots related to figure 6C.

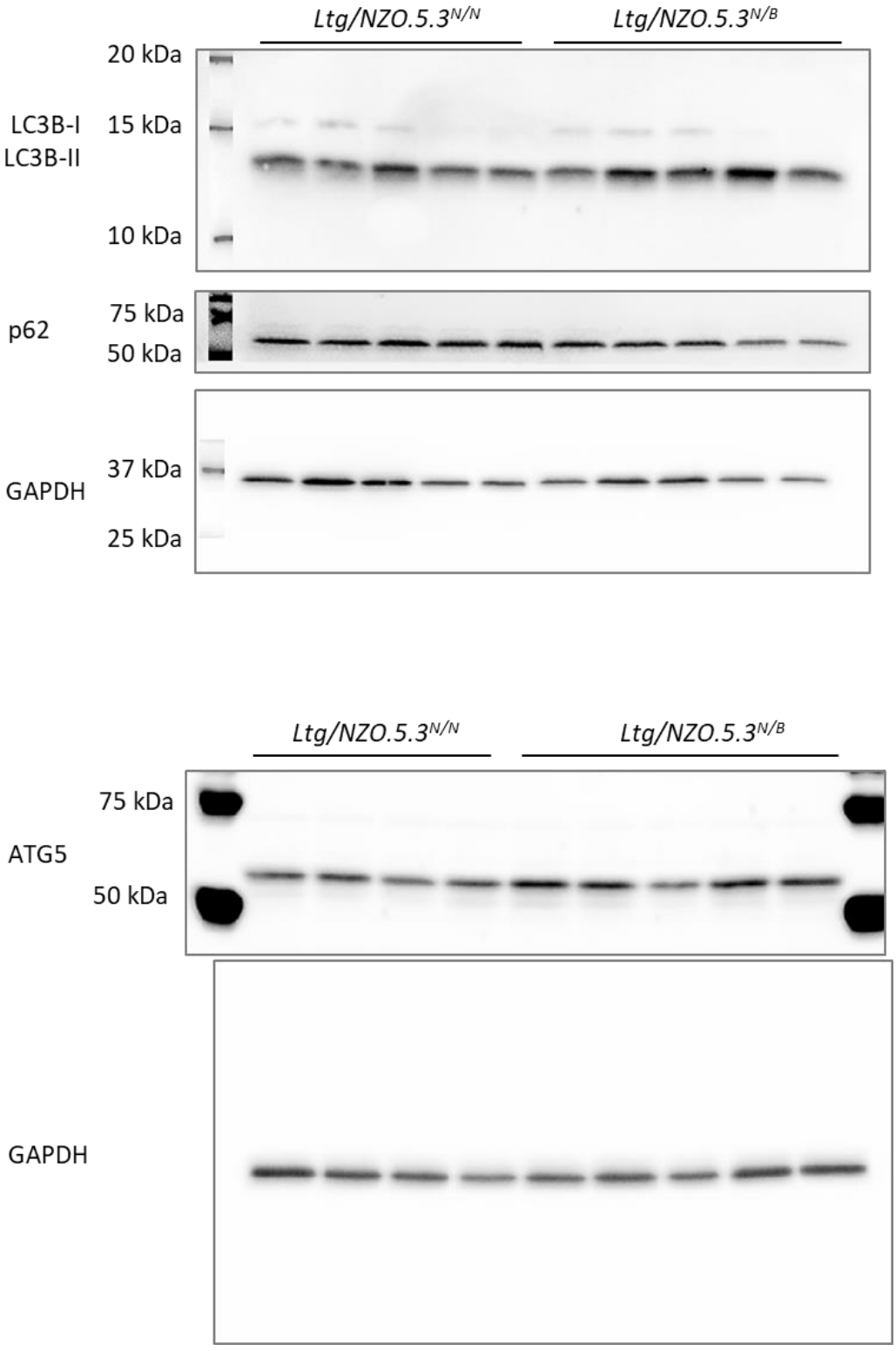

Fig. S17. Uncropped Western blots related to figure 6D.

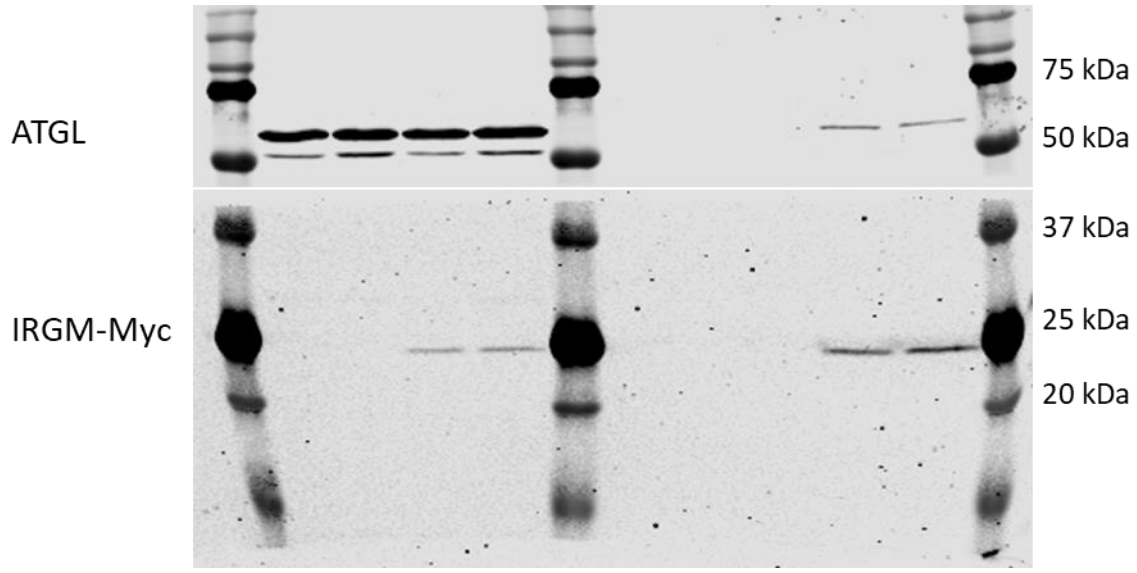

Fig. S18. Uncropped Western blots related to figure 7C.

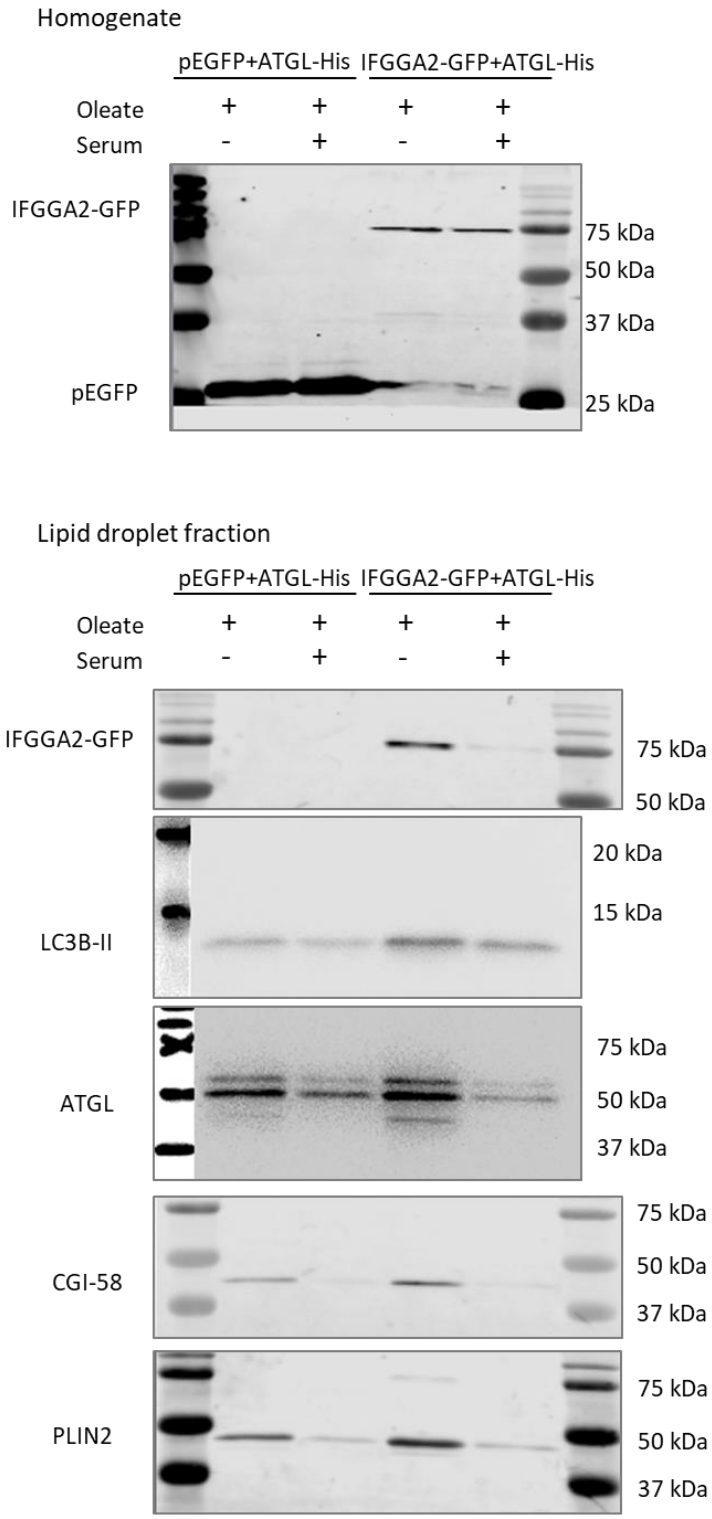

Fig. S19. Uncropped Western blots related to figure S9.

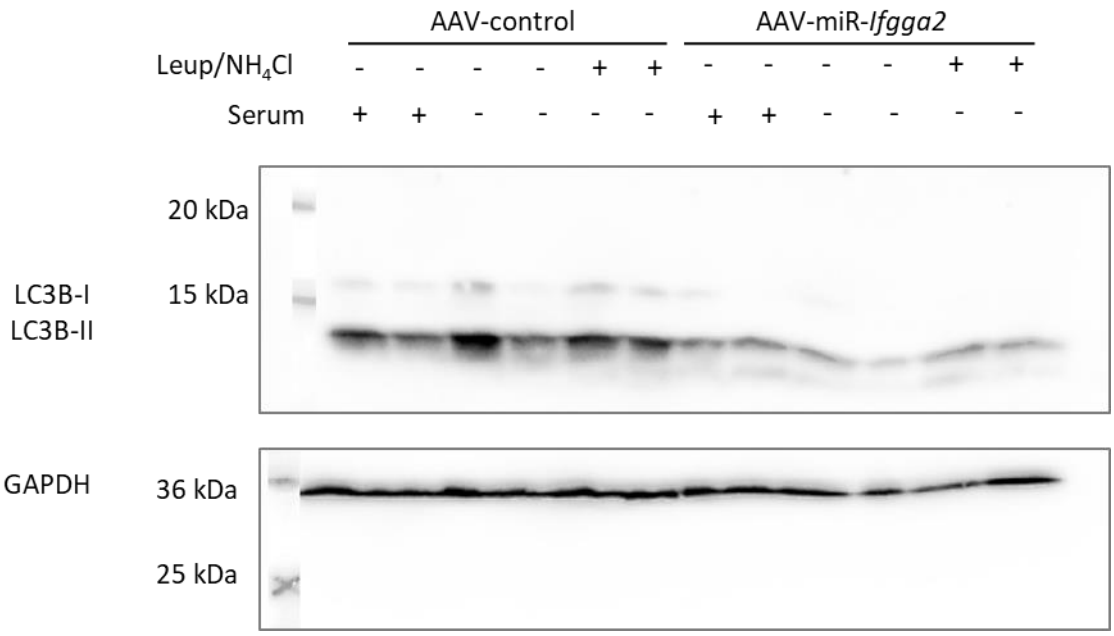

Fig. S20. Uncropped Western blots related to figure S11.

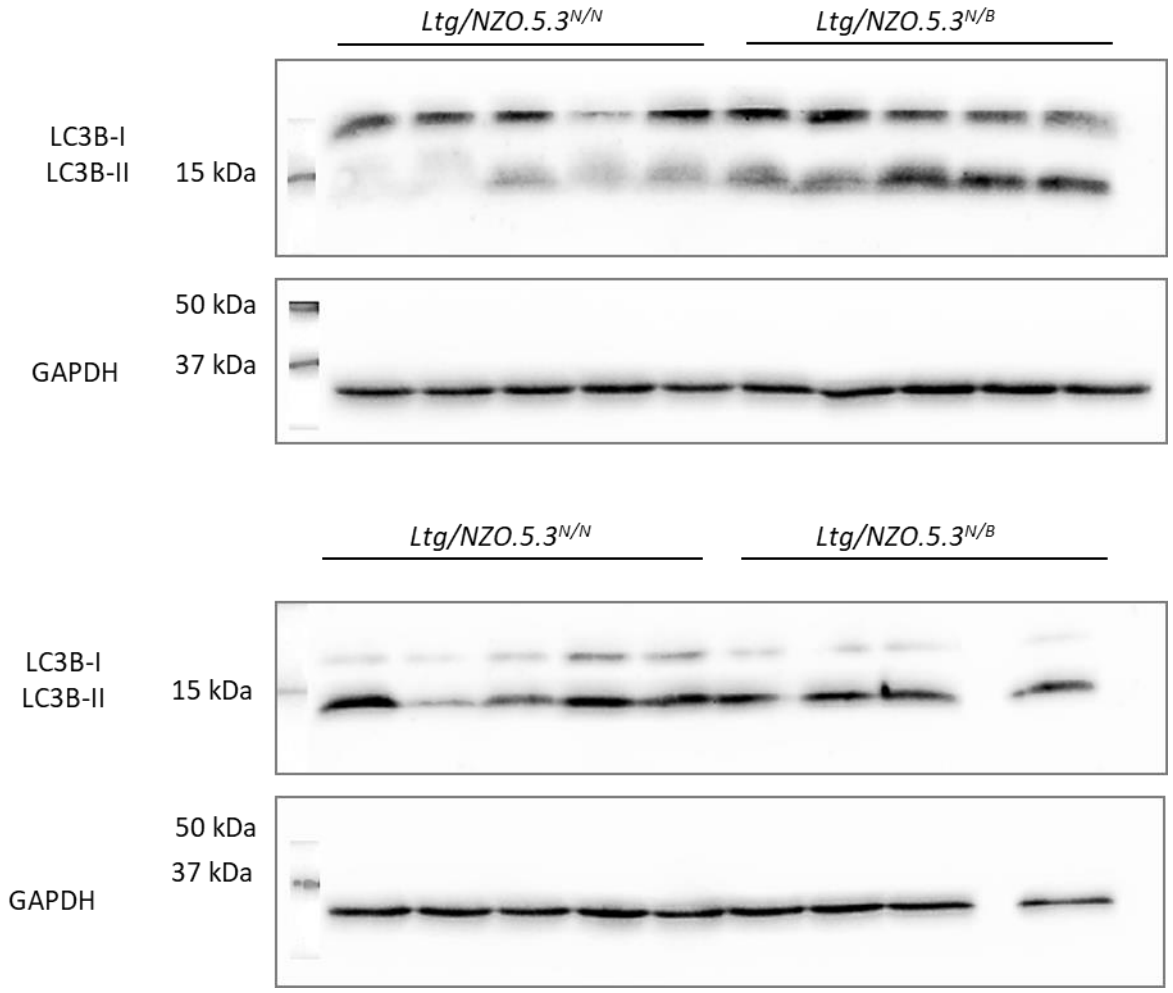

Fig. S21. Uncropped Western blots related to figure S12.

Supplementary tables

Table S1: Lipid concentrations in livers and plasma of *Ltg/NZO.5.3$^{N/N}$* and *Ltg/NZO.5.3$^{N/B}$* mice

	Ltg/NZO.5.3$^{N/N}$	***Ltg/NZO.5.3$^{N/B}$***		***Ltg/NZO.5.3$^{N/N}$***	***Ltg/NZO.5.3$^{N/B}$***
age 7 weeks, 16h fasted					
Liver triglycerides (µmol/ liver)	14.43 ± 4.35 n=7	5.958 ± 2.03 n=9 ***	Plasma triglycerides (mM)	1.805 ± 0.17 n=4	2.042 ± 0.49 n=5
			Plasma NEFA (mM)	0.60 ± 0.08 n=4	0.59 ± 0.16 n=5
			Plasma glycerol (mM)	0.437 ± 0.03 n=4	0.486 ± 0.11 n=5
			Plasma insulin (µg/l)	1.64 ± 0.79 n=4	1.36 ± 0.60 n=5

Data analyzed by unpaired *t*-test with Welch´s correction and presented as means ± SD. ***p<0.001.

Table S2: SNP markers for genotyping of the recombinant congenic mice

Chromosome	SNP ID	Mbp
18	*rs4231742*	*11.08*
18	*rs238887097*	*17.7*
18	*rs3705122*	*23.9*
18	*rs29718484*	*28.2*
18	*rs3654800*	*33.6*
18	*rs30259276*	*35.1*
18	*rs13464261*	*36.6*
18	*rs3693151*	*37.8*
18	*rs29932603*	*39.2*
18	*rs3683436*	*41*
18	*rs3683436*	*41.87*
18	*rs224675989*	*42.8*
18	*rs31955609*	*46.2*
18	*rs3713429*	*47.8*
18	*rs32089129*	*50.1*
18	*rs50578902*	*52.2*
18	*rs3706369*	*52.6*
18	*rs238770703*	*54.8*
18	*rs3721446*	*56.8*
18	*rs36491342*	*57.87*
18	*rs30170524*	*58*
18	*rs265444926*	*58.5*

Chromosome	SNP ID	Mbp
18	*rs46739734*	*58.8*
18	*rs3668927*	*59.2*
18	*rs50945333*	*62.5*
18	*rs3678144*	*62.9*
18	*rs252544110*	*63*
18	*rs30173956*	*63.3*
18	*rs3664098*	*63.5*
18	*rs30277652*	*63.9*
18	*rs30159308*	*64.1*
18	*rs262323405*	*64.5*
18	*rs234740351*	*64.8*
18	*rs4231907*	*65.1*
18	*rs3658391*	*65.8*
18	*rs3656892*	*68.9*
18	*rs3675825*	*70.85*
18	*rs3681034*	*71.9*
18	*rs3668697*	*74.9*
18	*rs3722222*	*75.6*
18	*rs3725940*	*77.9*
18	*rs3656292*	*79.7*
18	*rs238587725*	*82.4*
18	*rs29557756*	*84.8*
18	*rs3715760*	*87.5*

Table S3: Gene-specific primers for gene expression analysis using UPL.

Gene	Forward-Primer 5‘-3‘	Reverse-Primer 5‘-3‘	Probe
Brwd3	GTGAAACCTCCAAACGTGGT	GCGACTACATCCGGTTAATTG	#102
Dennd5b	GAGGCAACCAAAACTGTCAGA	CCAACATGCGTTTTGTCTTC	#62
Fubp1	AAAGTACCTCCCCAAAATGACTC	CTGGGACTTTGTATTCTTCTGTCA	#99
Hira	TTGCAACTGGAGGACAAGG	GGCAAAGCATCTTGGGAATA	#88
Krit1	GGGACTTCCTTTAGAAGTTGAGAA	TTGCCAGTGTTATCAGTTTAGCA	#17
Lmbr1	CAAGAGAAAATCCGATGAACAA	GAAGGTGCTCAGAAACAACGA	#89
Mmgt1	CCACTTGATAAATCTAGGCCATTT	GGAGGAAATCAGAGGTGACTACTAA	#55
Stam	TTGAGAAAGCAACTAGTGAGTTGAA	TGGAACGAAGACAATCTTTAGGTC	#73
Stat3	GGACCGTCTGGAAAACTGG	TCGCCCTTGTAGGACACTTT	#102
Tob1	ACTTTTGCTGCCACCAAGTT	GAGCTACCTTGCTGCTACGG	#22
Xrn1	AACAAGTCACGAGGCACATTT	TCGTTTCTTCTGGTGCACAT	#31

Table S4: Antibodies used for immunostaining.

Name	Supplier	Dilution	Cat. Number
ATGL	Abcam	1µg	ab220738
LAMP1	Developmental Studies Hybridoma Bank University of Iowa	1:100	H4A3
Rab11	Pierce/ Thermo Scientific	1:200	71-5300
Rab18	Protein Tech group	1:200	11304-ap
Transferrin receptor	Thermo Scientifiic	1:200	13-6800
PLIN2	Progen	1:500	GP40
PLIN2	Abcam	1:400	ab108323
LC3B	Cell Signaling	1:100	#2775
TO-PRO 3 iodide 642/661	Invitrogen	1:500	T3605
c-Myc	Clontech	1:600	631206
4,6-Diamidinon-2-phenylindo (DAPI)	Roche	1:1,000,000	10236276001
Anti-guinea pig Alexa 488	Thermo Fisher	1:200	A11073
Anti-mouse Alexa 488	Thermo Fisher	1:200	A11017
Anti-rabbit Alexa 647	Thermo Fisher	1:200	A-31573
Anti-mouse Alexa 594	Thermo Fisher	1:200	A-21203
Anti-rabbit Alexa 488	Thermo Fisher	1:200	A11070
Anti-mouse Alexa 568	Thermo Fisher	1:200	A11-004

Table S5: Antibodies used for Western blotting and co-immunoprecipitation.

Name	Supplier	Dilution	Cat. Number
ATGL	Cell Signaling	1:1,000	#2138
ATG5	Novus Biologicals	1:1,000	NB110-53818
P62	Progen Biotechnik GmbH	1:1,000	GP62-C
PLIN2	Progen	1:1,000	GP40
GAPDH	Ambion	1:25,000	AM4300
LC3B	Cell Signaling	1:1,000	#2775
GAPDH	Epitope Biotech Inc.		L001
Myc-Tag	Cell Signaling	1:500	#2772
Beclin1	Cell Signaling	1:1,000	3738
GFP	Santa Cruz	1:500	sc-9996
Anti-mouse POD	Dianova	1:20,000	315-035-008
Anti-rabbit POD	Dianova	1:20,000	111-035-003